Plankton Benthos Res 17(4): 369–382, 2022

Plankton & Benthos Research

Seasonal changes in taxonomic, size composition, and Normalised Biomass Size Spectra (NBSS) of mesozooplankton communities in the Funka Bay, southwestern Hokkaido: Insights from ZooScan analysis

Takumi Teraoka[1,*], Kanako Amei[1,2], Yutaka Fukai[1,3], Kohei Matsuno[4,5], Hiroji Onishi[4], Atsushi Ooki[4,5], Tetsuya Takatsu[4] & Atsushi Yamaguchi[4,5,*]

[1] *Graduate School of Fisheries Sciences, Hokkaido University, 3–1–1 Minato-cho, Hakodate, Hokkaido 041–8611, Japan*
[2] *Present Address: Atmosphere and Ocean Research Institute, The University of Tokyo, 5–1–5, Kashiwa, Chiba 277–8564, Japan*
[3] *Present Address: Kushiro Fisheries Research Institute, Hokkaido Research Organization, 2–6 Hamacho, Kushiro, Hokkaido 085–0024, Japan*
[4] *Faculty of Fisheries Sciences, Hokkaido University, 3–1–1 Minato-cho, Hakodate, Hokkaido 041–8611, Japan*
[5] *Arctic Research Centre, Hokkaido University, Kita-21 Nishi-11 Kita-ku, Sapporo, Hokkaido 001–0021, Japan*

Received 27 September 2021; Accepted 19 September 2022 Responsible Editor: Jun Nishikawa

doi: 10.3800/pbr.17.369

Abstract: Knowledge about the taxonomic and size composition of mesozooplankton is of critical importance for both fisheries and oceanography. In this study, we collected an annual time series of mesozooplankton samples in Funka Bay and analysed them using ZooScan to reveal the seasonal changes in taxonomic and size structure. Both zooplankton abundance and biovolume peaked in April and were dominated by an appendicularian *Oikopleura labradoriensis* which has been reported as being are being important food source for flatfish larvae. Furthermore, *Noctiluca scintillans* was abundant from September to December. The occurrence of this species may be related to the recent increase in the transport of Tsugaru Warm Current water into the bay. The Normalized Biomass Size Spectra (NBSS) was significant for 16 of 21 sampling dates. Insignificant NBSS, with an extremely flat slope, was observed for January–March. Significant NBSS with a flat slope was observed in April. Then, the relatively steep slopes of the NBSS were the case from mid-May to December. These seasonal changes in the slope of NBSS suggest that the energy transfer efficiency for higher trophic levels varied seasonally. The observed slopes of the NBSS in Funka Bay ranged from −1.09 to −0.30, which was flatter than the theoretical value (−1) and the previously reported values for the oceanic region of the western North Pacific. This suggests that the energy transfer e ciency to organisms at higher trophic levels in the Funka Bay is higher than in the adjacent oceanic region.

Key words: appendicularians, NBSS, *Noctiluca scintillans*, spring phytoplankton bloom, transfer e ciency

Introduction

Mesozooplankton serves as a food source for various commercially important organisms, and the size distribution of mesozooplankton is an important factor in determining the food selection of fish (Sheldon et al. 1977). The size composition of mesozooplankton also a ects the growth and mortality rates of the fish (Meeren & Næss 1993). Consequently, information on mesozooplankton is important for fisheries science. From an oceanographical viewpoint, the size distribution of the mesozooplankton community a ects the amount of material transported from the ocean surface to the deep layer via egested faecal pellets, a process called the biological pump (Michaels & Silver 1988, Ducklow et al. 2001). Thus, information on the size composition of mesozooplankton communities is of critical importance both in fisheries science (as a food source for fishes) and oceanography (with respect to material transfer cycles).

* Corresponding author: Takumi Teraoka; E-mail, takumi.terabyte74@gmail.com, Atsushi Yamaguchi; E-mail, a-yama@fish.hokudai.ac.jp

Traditionally, mesozooplankton size has been measured under a microscope, requiring much e ort and time. Consequently, studies on size composition were scarce, especially considering their importance. Recently a new instrument, ZooScan, has been developed to quantify mesozooplankton and provide data on size and taxon, by using image analysis (Gorsky et al. 2010). Since ZooScan can obtain taxonomic data as well as information on size, it is superior to the Optical Plankton Counter (OPC) (Herman 1988), which can only obtain data on size. With the widespread availability of these imaging analysis instruments, information on mesozooplankton in the field has accumulated rapidly (Vandromme et al. 2012, 2014, Marcolin et al. 2015a, 2015b, Romagnan et al. 2015, 2016).

The Normalized Biomass Size Spectra (NBSS) is commonly used to evaluate the size spectrum of mesozooplankton (Sprules & Munawar 1986, Zhou 2006, Zhou et al. 2009, Vandromme et al. 2014, Marcolin et al. 2015a). The NBSS is a regression-generated by plotting the mesozooplankton size on the *X*-axis and the standardized plankton biomass on the *Y*-axis and is used to assess the structure and trophic state of marine ecosystems (Platt & Denman 1977, 1978). The slope of the NBSS is a ected by both bottom-up and top-down controls (Platt & Denman 1977, 1978, Zhou 2006, Zhou et al. 2009). When the bottom-up controls dominate conditions due to nutrient increase and high productivity, the biomass of the small size classes of mesozooplankton increases. Consequently, the intercept of the NBSS increases, and the slope becomes steeper. However, under top-down conditions, since the large-body-sized mesozooplankton dominate, the intercept of the NBSS remains the same, but the slope becomes flattened (Moore & Suthers 2006). From field observations in the neighbouring waters of Japan, the slopes of the NBSS of the zooplankton samples collected by 335-μm mesh quantified by OPC have been reported to vary geographically (Fukuda et al. 2012, Sato et al. 2015) and seasonally (Hikichi et al. 2018). However, because of the scarcity of information on mesozooplankton NBSS, it is di cult to infer general changing patterns of mesozooplankton NBSS along with geographical and seasonal changes.

Funka Bay is located in the southwestern part of Hokkaido, Japan. It is a shallow (<100 m depth) bay and an important nursery area for various fish species such as walleye pollock (*Gadus chalcogrammus* Pallas, 1814) and flatfishes that spawn and feed there during larval and juvenile stages (Kamba 1977, Nakatani 1988, 2016, 2017, Nakatani & Maeda 1993, Hashimoto et al. 2011). The hydrographic characteristics of Funka Bay result from two di erent water masses (the Oyashio Cold Current and the Tsugaru Warm Current) that intrude into the bay, and which water mass dominates varies with the season (Ohtani 1971, Ooki et al. 2019). In response to seasonal changes in the physical oceanography, zooplankton communities also show great seasonal fluctuations (Hirakawa 1976, 1979, 1983). In addition to changes in community structure, seasonal changes in the various dominant mesozooplankton taxa have also been reported (Dohi 1982, Shiga 1985, Yokouchi 1985, Yamaoka et al. 2019). Such information is important, which makes it unfortunate that no data are available on the size structure and NBSS of the mesozooplankton and their seasonal changes.

It should also be noted that water temperatures in Funka Bay have been warmer recently, which may be related to climate change (Ooki et al. 2019). The volume of the Tsugaru Warm Current transported from the Japan Sea through the Tsugaru Strait is reported to be increased during 1996–2012 (Kida et al. 2021). In Funka Bay, due to the warming, the water mass classifications dating from the 1960s and 70s (Ohtani 1971) are outdated, and new water mass classifications have been established recently (Ooki et al. 2019). Such warming is expected to a ect marine ecosystems, but as yet, little information is available on the changes observed in the mesozooplankton community resulting from the warming.

In this study, we analysed a time series of mesozooplankton samples collected at one station in the central section of Funka Bay from December 2018 to December 2019. We collected the mesozooplankton using a plankton net with a fine mesh (100 μm) in order to collect the whole mesozooplankton community. The mesozooplankton samples were preserved in formalin and subsequently analysed by ZooScan for taxonomic and size information along with abundance and biovolume. The taxonomic information obtained was then compared with the taxa recorded in the mesozooplankton communities in the 1980s (Hirakawa 1983, Shiga 1985). We compared the NBSS data of the zooplankton samples collected by 335-μm mesh net and quantified by OPC from around Hokkaido with those from the oceanic region of the western North Pacific (Fukuda et al. 2012, Shiota et al. 2013, Sato et al. 2015, Hikichi et al. 2018, Mishima et al. 2019). It should be noted that we used a zooplankton net with 100-μm mesh size and quantified samples by ZooScan in this study. To make quantitative/qualitative comparison possible with the previous studies, we calculated NBSS based on the size ranges of 350-μm to 5-mm which is the same as in the previous studies. Through this comparison, we evaluated general changing patterns in terms of the geographical (coastal vs. oceanic) or seasonal changes in the NBSS.

Materials and Methods

Field sampling and hydrography

We sampled mesozooplankton at a quasi-monthly interval from 12 December 2018 to 16 December 2019 using a North Pacific Standard (NORPAC) net (mouth diameter 45 cm, 100 μm mesh) deployed to near the bottom (87± 2 m [mean±sd]) and towed vertically 21 times at Sampling Station 30 (St. 30), located at the centre of Funka Bay (depth: 95 m) (Fig. 1). The filtration volume of the net

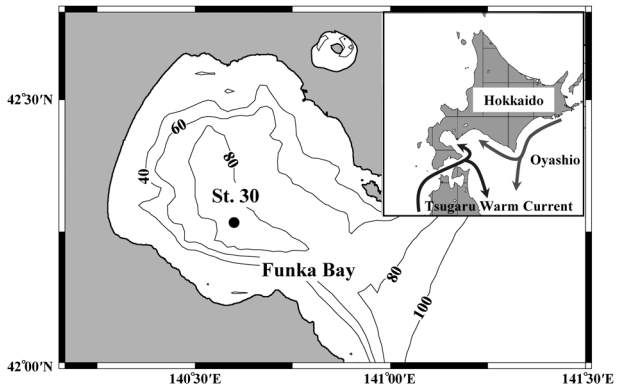

Fig. 1. Location of the sampling station (St. 30) at the center of Funka Bay, southwestern Hokkaido, Japan. Directions of the currents are shown by the arrows in the upper-right panel. Depth contours are superimposed on the main panel.

was 11.9±2.4 m^3, and the mean filtration e ciency was 86%. The collected mesozooplankton samples were preserved with 5% v/v borax-bu ered formalin seawater. At each sampling, water temperature and salinity were measured using a conductivity-temperature-depth (CTD) probe (SBE 19plus, Sea-Bird Scientific Inc.). To identify the water masses, T-S diagrams were made. For the classification of water masses, we referred to Ooki et al. (2019). Using the seawater samples from 0, 5, 10, 20, 30, 40, 50, 60, 70, 75, 80, and 85 m that were collected by a bucket (0-m) or the rosette-mounted Niskin bottles on the CTD, nutrient concentrations (NO_3^- and NO_2^-) were measured by the colorimetric method using a QuAAtro system (BL-Tec, Osaka, Japan). Chlorophyll *a* concentrations in the seawater samples (100 mL) were measured by the Welschmeyer method (Welschmeyer 1994) using a fluorometer model 10-AU-005 (Turner Designs, San Jose, CA, USA).

ZooScan analysis

In the laboratory, zooplankton images were scanned with a ZooScan system (Hydrooptic Inc.) based on the method of Gorsky et al. (2010). Before each measurement, background measurements were made with deionised water. Zooplankton subsamples of 1/3 to 1/90 (depending on the amount of the sample) were made by a wide-bore pipette and scanned. The obtained images were separated into individual images using the ZooProcess software. The zooplankton images were digitised at 2400 dpi resolution, at which one pixel corresponded to 10.6 μm. The obtained images were uploaded to the website Ecotaxa (http://ecotaxa.obs-vlfr.fr/prj/). The identification of each taxon was made semi-automatically through the web (Picheral et al. 2017). The taxonomic groups and species identifications in this study included the large copepod *Eucalanus bungii* Giesbrecht, 1893, *Metridia pacifica* Brodsky, 1950, *Neocalanus* spp., other members of Copepoda, Euphausiacea, Appendicularia, Chaetognatha, Polychaeta, Amphipoda, Cnidaria, Thaliacea, *Noctiluca scintillans* (Macartney) Kofoid & Swezy, 1921 (hereafter we termed *Noctiluca*), benthos larvae, and detritus. Within them, detritus was excluded from subsequent analyses because it is a non-living fraction.

ZooScan provides estimates of body length (major axis of the best fitting ellipse) and width (minor axis) (Gorsky et al. 2010). The volume of the ellipse (*Volume,* mm^3) was calculated using the major axis length (L_{major}, mm) and the minor axis width (L_{minor}, mm) (Vandromme et al. 2012):

$$Volume = 4/3 \times \pi \times (L_{major}/2) \times (L_{minor}/2)^2$$

From the volume of the ellipse, the Equivalent Spherical Diameter (ESD, mm) with the same volume was calculated:

$$ESD = \sqrt[3]{\frac{Volume \times 3}{4\pi}}$$

The abundance (*N*: ind. m^{-3}) was calculated from the number of particles (*n,* where *n* is the number of particles in each size class every 0.05 mm between 0.2 and 5.0 mm ESD) and the volume of filtered water (*F*: m^{-3}). The biovolume (*B*: mm^3 m^{-3}) was also calculated from the volume (mm^3) and *F* using the following equation:

$$N = \frac{n}{F \times s}$$

$$B = \frac{Volume}{F \times s}$$

where *s* is the split factor of the ZooScan measurement.

Zooplankton community

To evaluate the trends of the mesozooplankton community structure, cluster analysis based on their abundance was conducted. Cluster analysis was performed by connecting the Bray-Curtis similarities using the mean linkage method based on the standardised log (*X*+1) values of the abundance data (*X*: ind. m^{-3}) of each zooplankton taxon in each sample. Di erences in abundance between the communities were tested by one–way ANOVA and the Tukey–Kramer test. These statistical analyses were performed using the Primer 7 software package (Primer-E, Ltd., Quest Research Limited, Albany, Auckland, New Zealand) and StatView 5.01 (SAS Institute Inc., Cary, NC, USA).

To evaluate the relationship between environmental parameters and the zooplankton community, a distance-based linear modelling (DistLM) and a distance-based redundancy analysis (dbRDA) were carried out. All environmental parameters were normalized, and then the DistLM was run with dbRDA plot by combining the resemblance matrix (based on Bray-Curtis similarities between the abundances of zooplankton species in the samples) and the hydrographic variables (including slope and intercept from NBSS). To run DistLM, we choose "All specified" as a selection procedure, "R^2" as a selection criterion, and the

number of permutations was 999. The analyses were conducted using the Primer 7 software.

NBSS

For NBSS analyses, although we used a plankton net with a mesh size of 100 μm, to make an adequate comparison with the previous studies that used a 335 μm mesh net, we used only the data with>0.35 mm ESD for the NBSS calculation. The biovolume (mm^3 m^{-3}) summed at each 0.05 mm between 0.35 and 5.0 mm ESD was used for the data of the NBSS analysis. These size categories were the same as the previous studies (Fukuda et al. 2012, Shiota et al. 2013, Sato et al. 2015, Hikichi et al. 2018, Mishima et al. 2019). The *X*-axis of the NBSS is the biovolume of each size class transformed to the normal logarithm (*X*: $\log_{10}$ zooplankton biovolume [mm^3 ind^{-1}]), and the *Y*-axis is the biovolume of each size class divided by the di erence in biovolume between adjacent size classes (Δbiovolume [mm^3]). (*Y*: $\log_{10}$ zooplankton biovolume [mm^3 m^{-3}]/ Δbiovolume [mm^3]). The linear equation of NBSS was obtained using the MS Excel solver function:

$$Y = aX + b$$

where *a* and *b* are the slope and intercept of the NBSS, respectively. To clarify the interaction between slope (*a*) and intercept (*b*) of the NBSS, we made a scatter plot between them.

Results

Hydrography

Water temperatures ranged from 2.1 to 20.5℃ throughout the entire period (12 December 2018 to 16 December 2019) at St. 30 in Funka Bay (Fig. 2a). From February to March, the temperatures were vertically uniform and decreased to 3–4℃ in this period. However, after April, water temperature increased in the epipelagic zone, and the development of the thermocline was observed at a depth of approximately 40 to 50 m from August to October.

Salinity ranged from 30.0 to 34.1 but was high (>33.8) and vertically uniform from December to February (Fig. 2b). After March, low salinity was observed in the epipelagic zone. A low-salinity water (<32.4) was observed at depths shallower than 30 m from May to August.

Nutrients (NO_3^-+NO_2^-) ranged from 0.05 to 18.88 μM L^{-1}

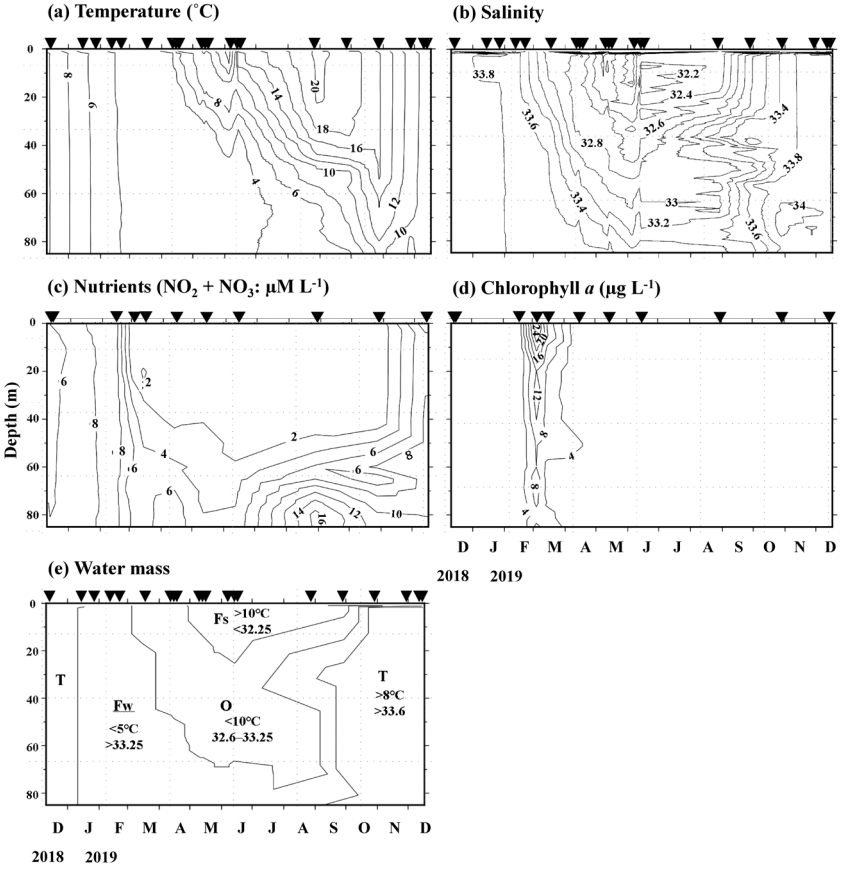

Fig. 2. Seasonal changes in temperature (a), salinity (b), nutrients (c), chlorophyll *a* (d), and water mass (e) at St. 30 in Funka Bay, southwestern Hokkaido, Japan, from December 2018 to December 2019. Triangles at the top abscissa indicate sampling dates. Water mass classifications are derived from Ooki et al. (2019). T: Tsugaru Warm Current, Fw: Funka Bay water formed in winter, O: Oyashio Coastal Branch, Fs: Funka Bay water formed in summer.

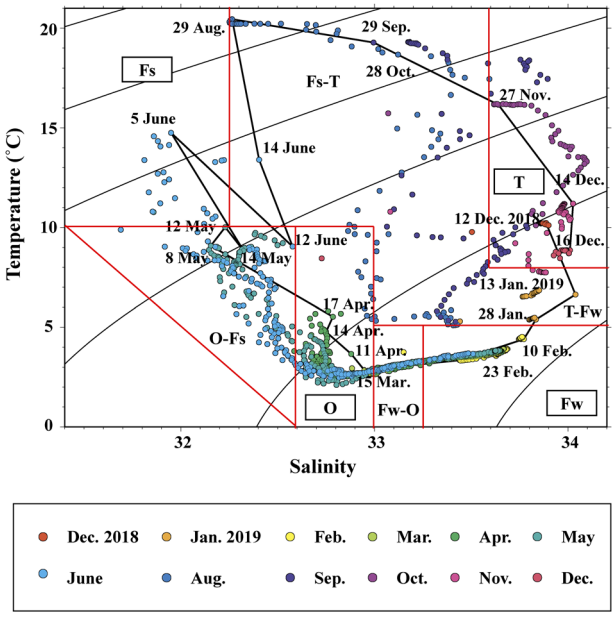

Fig. 3. Seasonal changes in Temperature-Salinity diagrams at St. 30 in Funka Bay, southwestern Hokkaido, Japan, from December 2018 to December 2019. Black lines denote seasonal changes in properties at the sea surface. Red lines represent water masses. Water mass classifications are derived from Ooki et al. (2019). O: Oyashio Coastal Branch, Fs: Funka Bay water formed in summer, T: Tsugaru Warm Current, Fw: Funka Bay water formed in winter.

and were vertically uniform from December to February (Fig. 2c). From the end of February to early March, the nutrients above 40 m rapidly decreased from 8 to<2 μM L^{-1}. The lowest nutrient concentration (<2 μM L^{-1}) was observed for the upper 40 m of the station during the long period between March and October.

Chlorophyll *a* concentrations ranged from 0.00 to 29.71 μg L^{-1} and were high for a temporally restricted period: from the end of February to mid-April (Fig. 2d). For the other periods, high chlorophyll *a* concentrations (>4 μg L^{-1}) were not detected.

The plot positions in the T–S diagram varied greatly within each water mass (Fig. 3). Four water masses were identified in Funka Bay, namely: Funka Bay water formed in winter (Fw), Oyashio Cold Current water (O), Funka Bay water formed in summer (Fs), and Tsugaru Warm Current water (T) (Fig. 2e). In addition, the transitions between them from mixing processes, such as Fw–O and Fs–T, are also present, as were the transitions resulting from warming or cooling processes within the water masses, such as O–Fs and T–Fw (Ohtani 1971, Ooki et al. 2019). During the study period, the Tsugaru Warm Current was observed in December 2018, and its cooling process (T–Fw) occurred in January 2019. Fw dominated in February and was subsequently replaced by the Oyashio Cold Current in March–April; its warming process (O–Fs) in turn was seen in May. During June and August, Fs dominated, and the mixing process of the two water masses (Fs–T) occurred in September-October. Finally, the Tsugaru Warm Current dominated the following December again. Thus, within the annual scale, clockwise changes were observed for the plotted positions in the T–S diagram (Fig. 3).

Zooplankton abundance and biovolume

The total zooplankton abundance and biovolume ranged from 255 to 3,467 ind. m^{-3} and 12 to 2,034 mm^3 m^{-3}, respectively (Fig. 4). Seasonal changes in abundance and biovolume varied with taxa, and four seasonal patterns of change were detected. The first pattern was forming abrupt abundance peaks in April, which was observed for the copepods *M. pacifica* and *Neocalanus* spp., as well as for Euphausiacea, Appendicularia, Polychaeta, and Amphipoda. The second pattern was abundant between April and June, which was observed for the copepod *E. bungii* and the other Copepoda. The third pattern was abundant during June-December, including Chaetognatha and Cnidaria. The fourth pattern was abundant from September to December and not detected for the other periods, observed for Thaliacea and *Noctiluca*.

Zooplankton communities

The cluster analysis based on zooplankton abundance separated the zooplankton community into three groups at 73.1% dissimilarity (Fig. 5a). The remaining four samples were treated as an "out-group". Each group contained 4 to 9 samples. We termed the three groups A, B, and C. The occurrence period of each group was separated clearly: Group A was seen from August to January, Group B occurred from December to February, and Group C appeared from April to June. For taxonomic accounts, the occurrence pattern of each taxon was classified into seven groups at 89.8% dissimilarity. Within them, for the taxonomic groups including several taxa, large copepods such as *Eucalanus bungii*, *Metridia pacifica*, *Neocalanus* spp., and polychaetes occurred dominantly in Group C. For the remaining taxa, it should be noted that *Noctiluca* occurred in great numbers in Group A. Inter-group di erences in abundance were tested by one–way ANOVA and the Tukey–Kramer test (Table 1). For the taxa, two species/taxa exhibited significantly di erent abundances between the groups: *E. bungii*, a large copepod, was abundant in Group C, and *Noctiluca* was present in high numbers in Group A.

Results of dbRDA indicated that the zooplankton community in the Funka Bay could be classified from the *X*-axis (dbRDA 1) representing changes in temperature and the *Y*-axis (dbRDA 2) indicating NBSS intercept (Fig. 5b). Contributions for the variation of each axis were similar (35.0% and 21.4%), and it should be noted that these two axes contributed a relatively high component (>50%) of the variations. From the result of DistLM, four environmental parameters (temperature, salinity, NBSS intercept and slope) explained 65.7% of the zooplankton variation.

Within the dbRDA plots, the large changes in the plotted

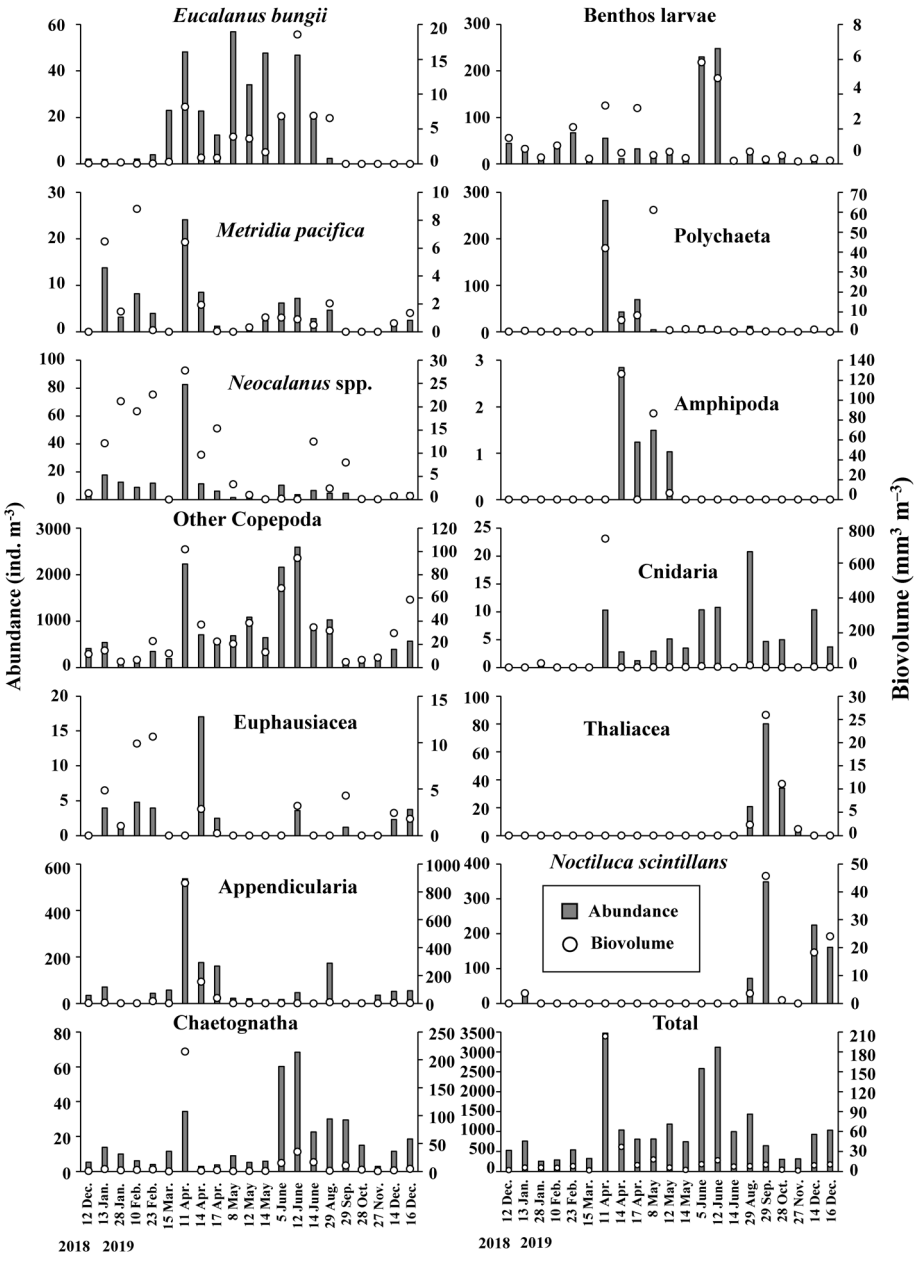

Fig. 4. Seasonal changes in abundance and biovolume of each zooplankton taxon at St. 30 in Funka Bay, southwestern Hokkaido, Japan, from December 2018 to December 2019.

area were observed on two occasions: 14 June to 29 August and 15 March and 11 April (Fig. 5b). For the changes from 14 June to 29 August, the changes in the plotted area were seen along the *X*-axis (dbRDA 1). This change represented the community change from Group C to Group A. While for the other large changes from 15 March to 11 April, their changes were observed along the *Y*-axis (dbRDA 2). It should be noted that the zooplankton community of Group C was plotted at the left end of the dbRDA plots but has a large plotted area vertically within the same Group C (Fig. 5b).

NBSS

Significant NBSS with a negative slope was observed for 16 of the 21 sampling dates (r^2=0.33–0.90, $p < 0.05$; Fig. 6). The periods when NBSS was not significant were restricted from 28 January to 15 March, and most of them belonged to Group B. During that period, the slopes of the NBSS were extremely flat. For the dates showing a significant NBSS, the slope of the NBSS ranged from −1.09 to −0.30. Flat slopes of NBSS (−0.63 to −0.29) were observed for 11–17 April belonging to Group C. These dates were characterized by the high biovolume of Appendicularia (Fig. 4). On the other hand, the slopes were steeper for the rest of the season: mid-May to January, ranging

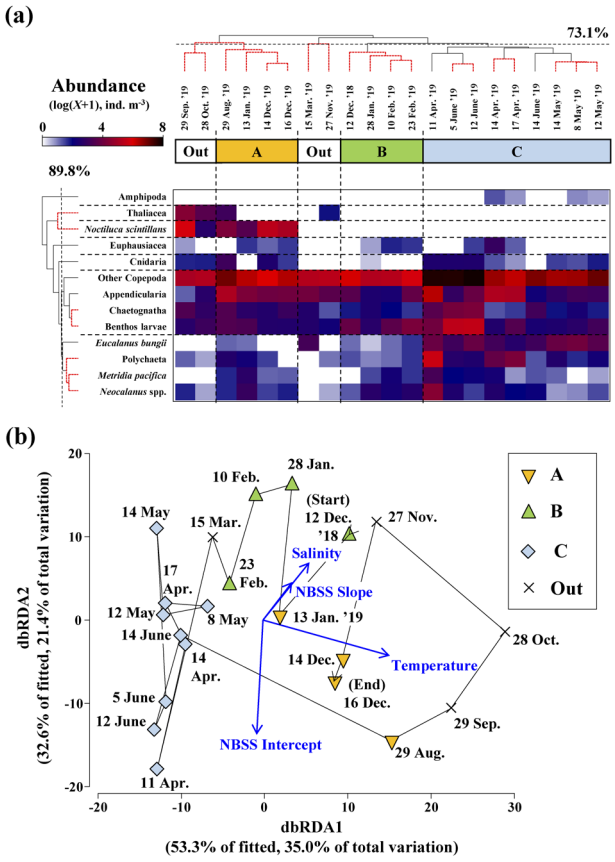

Fig. 5. Result of cluster analysis based on the mesozooplankton abundance at St. 30 in Funka Bay, southwestern Hokkaido, Japan, from December 2018 to December 2019 (a). Dashed lines represent significant divisions for the taxon (horizontal axis) and sampling dates (vertical axis). dbRDA plots of the three groups (A–C) with environmental parameters (b). The arrowhead direction and length of the arrow lines in the middle of the panel indicate the relationship between groups and the strength of the parameters. The slope and intercept of the NBSS were referred from Fig. 6.

from −1.09 to −0.63. The intercept of NBSS ranged from 0.273 to 2.101.

Based on the data from the whole study period, there was a significant positive relationship between the slope and intercept of the NBSS (r^2=0.28, $p < 0.05$; Fig. 7). This significant relationship was also the case by eliminating the five dates of insignificant NBSS (r^2=0.55, $p < 0.05$). Within the scatter plots between slope and intercept of NBSS, the plotted area varied with the zooplankton community. Thus, zooplankton in Group A were settled in the middle of the scatter plot. Insignificant NBSS (underlined dates in Fig. 7) was mostly observed for the zooplankton in Group B. The largest variabilities of the plotted area were seen for the zooplankton in Group C.

Seasonal changes in the zooplankton community

Seasonal changes in water mass, zooplankton community, zooplankton abundance, biovolume, and slope and intercept of NBSS during the study period are summarized in Fig. 8. For the zooplankton in Group A, both abundance and biovolume were stable and similar within the community. For the zooplankton in Group B, the slope and intercept of the NBSS in December greatly varied from the other dates, but for the other dates, slopes were extremely flat, resulting in insignificance of NBSS. The greatest differences in NBSS within the same zooplankton community were seen for the zooplankton in Group C observed from April to June. For April, the slopes of NBSS were flat, then having insignificant NBSS on 8 May, after that, the slopes of NBSS showed steep slopes (−0.99 to −0.75) for other dates.

Discussion

Seasonal changes in zooplankton communities

Both zooplankton abundance and biovolume peaked in April (Fig. 8), which is consistent with previous reports regarding zooplankton abundance and biomass around Hokkaido peaking in spring (Ban et al. 1998, Yamaguchi et al. 2003, 2014, Shimada et al. 2012, Arima et al. 2014a, Hirakawa et al. 2019). This is a result of the abundant spring bloom of phytoplankton occurring approximately one month earlier than that time (Fig. 2d). Consequently, the numerically dominant small copepods reproduce, and growth takes place simultaneously in the biomass-dominant large copepods such as *Neocalanus* spp. (Yamaguchi & Shiga 1997, Shimada et al. 2012, Arima et al. 2014a, 2014b, Kitamura et al. 2016). In this study, the numerically dominant taxa were "other Copepoda". The species belonging to this category are *Pseudocalanus* spp. and *Paracalanus* spp., and both are known to be abundant throughout the year (Yamaguchi & Shiga 1997, Ban et al. 1998, Yamaguchi et al. 2003).

The dominant appendicularian during April, when whole zooplankton abundance and biovolume are high, has been reported to be the cold-water species *Oikopleura labradoriensis* Lohmann, 1892 (Shiga 1985, Yamaoka et al. 2019). In Funka Bay, the cold-water species *Fritillaria borealis* Lohmann, 1896 is also abundant, especially in the Fw and O water masses (Shiga 1985). Of these, the larger *O. labradoriensis* is abundant by biovolume in spring (Teraoka unpublished). In various subarctic regions of the northern hemisphere, appendicularians are known to have high filtering rates and productivity, and their discarded houses play an important role in vertical material transport (Alldredge 1976, Flood 1991, Choe & Deibel 2008, Doubleday & Hopcroft 2015). In Funka Bay, the dominant appendicularian, *O. labradoriensis*, is reported to be an important food source for the larvae of the flathead flounder (*Hippoglossoides dubius* Schmidt, 1904) and the stone flounder (*Platichthys bicoloratus* [Basilewsky, 1855]) from January to May (Miyamoto et al. 1993, Hashimoto et al. 2011). It also should be noted that appendicularians have the ability to feed on small particles by filtering ambient

Table 1. Inter-group differences in the abundance of each taxon or species of the three groups of mesozooplankton separated by Bray–Curtis similarity (cf. Fig. 5a) in Funka Bay from December 2018 to December 2019.

Taxa/species	Mean abundance (ind. m^{-3})			one-way
	A (4)	B (4)	C (9)	ANOVA
Eucalanus bungii	1.07[a]	2.14[a]	34.47[b]	***
Metridia pacifica	5.80	3.82	5.94	NS
Neocalanus spp.	7.69	8.99	14.06	NS
Other copepods	632.3[a,b]	286.59[a]	1277.45[b]	*
Euphausiacea	2.49	2.44	2.57	NS
Appendicularia	87.64	24.37	111.47	NS
Chaetognatha	18.49	6.34	23.58	NS
Benthos larvae	20.07	40.18	70.39	NS
Polychaeta	5.72	2.62	49.41	NS
Amphipoda	0	0	0.73	NS
Cnidaria	8.72	0.13	5.25	NS
Thaliacea	5.20	0	0	NS
Noctiluca scintillans	122.77[b]	0[a]	0[a]	**
Others	122.77	26.08	43.80	NS
Total	1039.62	403.72	1639.11	NS

Values in parentheses indicate the number of samples included in each group. Differences were tested by one-way ANOVA and Tukey–Kramer tests. Results of the Tukey–Kramer test are shown by differences in superscript alphabets ($p < 0.05$). NS: not significant *: $p < 0.05$; **: $p < 0.01$; ***: $p < 0.001$.

water (Alldredge 1976, Flood 1991, Choe & Deibel 2008, Doubleday & Hopcroft 2015). These facts suggest that the appendicularian *O. labradoriensis* probably plays an important role in material transfer connecting the productivity of the spring phytoplankton bloom to the higher trophic levels in the spring marine ecosystem of Funka Bay. The other abundant taxa in this period included Polychaeta, Amphipoda, Euphausiacea, and the copepods *M. pacifica* and *Neocalanus* spp. (Fig. 4). All of these are cold-water taxa, having large body sizes, and are expected to be highly nutritional food for higher trophic level organisms.

For the dominant taxa of summer to autumn, *Noctiluca* stood out. While *Noctiluca* has not previously been reported to be dominant in Funka Bay (cf. Hirakawa 1983), they are reported to dominate in warm water masses such as the Kuroshio and the Tsushima Warm Current (Miyaguchi et al. 2006, Ara et al. 2013, Suzuki et al. 2013). In the present study, *Noctiluca* were limited to Fs–T and T water masses, which indicates that this genus was transported by the Tsugaru Warm Current. It is interesting to note that, while Fw is the cooled Tsugaru Warm Current (Ohtani 1971, Ooki et al. 2019), no *Noctiluca* were observed in Fw after December, suggesting that *Noctiluca* died out under such cold conditions (Fig. 4). In recent years, warming trends have been reported for Funka Bay (Ooki et al. 2019). A yearly increasing trend of the amount of the Tsugaru Warm Current transported has been reported for 1995–2012 (Kida et al. 2021). The dominance of warm-water *Noctiluca*, which has never been reported previously, during the warm season in Funka Bay is noteworthy as an effect of climate change on the zooplankton community in Funka Bay.

In this study, the zooplankton community in Funka Bay was classified into three major groups, of which three groups (A, B, and C) occurred clearly separated by season (Fig. 8). Concerning Group C, temporal variability of the plotted area in dbRDA plot was prominent for Group C (Fig. 5b). In the dbRDA plot, the plotted area of Group C lay on the left side (low dbRDA1) but had high variability along the *Y*-axis (dbRDA2). In fact, for the three dates plotted in the lower-left corner of the dbRDA plot (11 April, 5 June, and 12 June), the abundances of the other Copepoda, Appendicularia, Chaetognatha, and benthos larvae were the highest (Fig. 5a). On the other hand, within Group C, for the four dates characterized with a positive dbRDA2 (17 April, 8, 12, 14 May), the abundances of the above taxa were relatively low (Fig. 5a). Based on the five-years of observations in Funka Bay, the spring phytoplankton bloom has been reported to occur in March-April (Kudo & Matsunaga 1999) which corresponds with that also observed in this study (the end of February to mid-April) (Fig. 2d). As a mechanism for the initiation of the spring phytoplankton bloom in Funka Bay, intrusion of the Coastal Oyashio Water is important (Shinada et al. 1999a). During spring, the magnitude of the phytoplankton bloom exhibited great spatiotemporal changes (Sasaoka et al. 1998, Shinada et al. 1999b). Under such conditions, such large spatiotemporal variability is also expected to be present in the zooplankton community. Thus, large variabilities in dbRDA2 observed for the zooplankton in Group C would be a reflection of the spatiotemporal changes in the zooplankton community. These phenomena would be related to the bot-

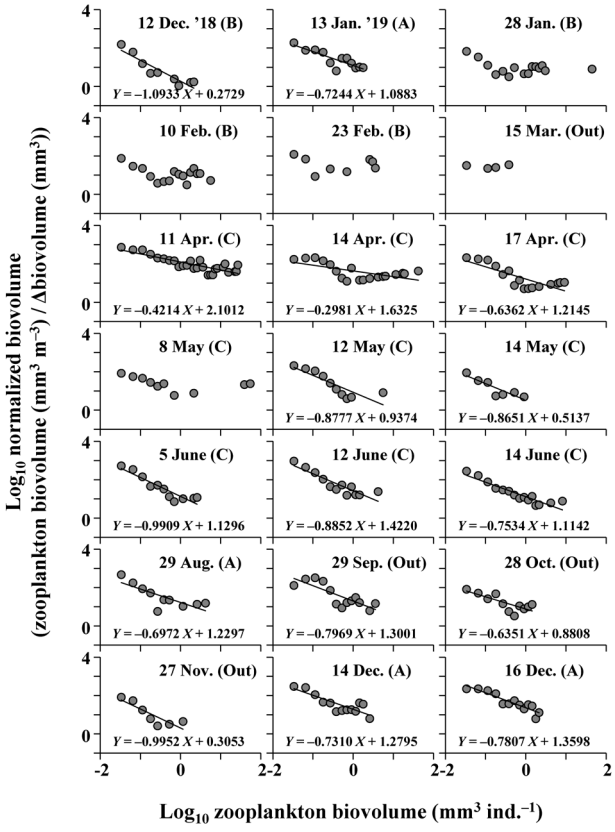

Fig. 6. Seasonal changes in normalised biomass size spectra (NBSS) at St. 30 in Funka Bay, southwestern Hokkaido, Japan, from December 2018 to December 2019. Note that, except for five sampling dates (28 January, 10 and 23 February, 15 March and 8 May 2019), NBSS regressions are highly significant (r^2=0.40–0.87, $p < 0.05$). The alphabets in the parentheses indicate zooplankton community groups identified from the cluster analysis (cf. Fig. 5a). Out: out-group.

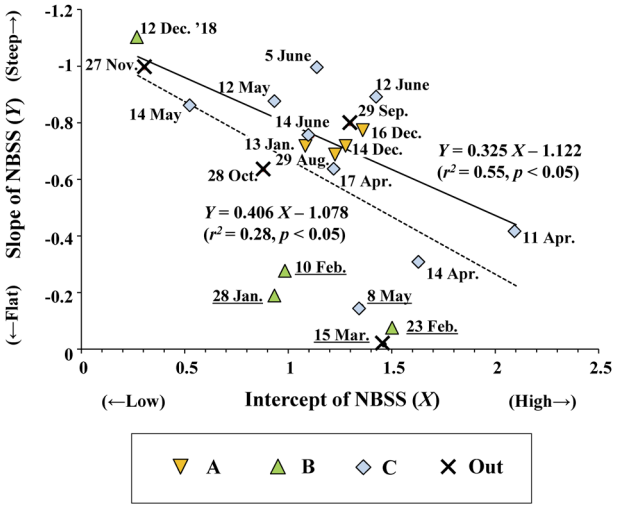

Fig. 7. Relationship between slope and intercept of normalised biomass size spectra (NBSS) derived from mesozooplankton in Funka Bay, southwestern Hokkaido, Japan, from December 2018 to December 2019. Di erences in symbols (A, B, C, and Out) represent di erences in the zooplankton community (cf. Fig. 5a). Five dates with underlines indicate the insignificance of NBSS (cf. Fig. 6). Dashed and solid lines represent significant relationships between slope (Y) and intercept (X) of NBSS based on the whole data set (dashed line) and only for the significant NBSS data (solid line), respectively.

tom-up e ect of the primary productivity, which exhibited large spatiotemporal changes (Sasaoka et al. 1998, Shinada et al. 1999b).

For the zooplankton community in Group A, the large changes along the X-axis in dbRDA1 between 14 June and 29 August were induced by the changes in the zooplankton community from Group C to Group A (Fig. 5b). The di erences in the dominant zooplankton taxa between the two groups were *E. bungii*, Polychaeta, *M. pacifica*, and *Neocalanus* spp. for Group C, while Thaliacea and *Noctiluca* dominated Group A (Fig. 5a). Note that the dominance of Thaliacea was observed only from August to October. The dominant water masses in the period where Group A dominated were S, S-T, and T. Under such warm conditions, development of the thermocline occurred (Fig. 2a), and primary productivity was expected to be low, considering the chlorophyll *a* data (Fig. 2d). With such low primary production and stable conditions, zooplankton is also expected to be in a stable state. These facts suggest the dominance of a complex planktonic food-web during this season. Combining such a complex food-web struc-

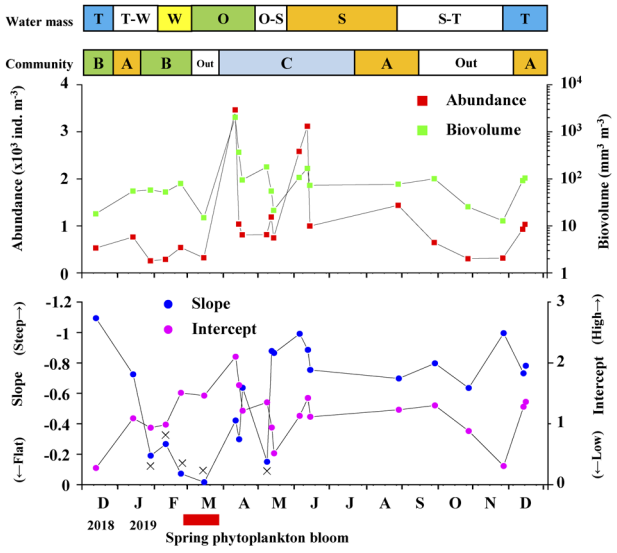

Fig. 8. Summary panels on seasonal changes in water mass, mesozooplankton community classification based on abundance (cf. Fig. 5a) (upper panels), abundance and biovolume (middle panel), and slope and intercept of normalised biomass size spectra (NBSS) (cf. Fig. 6) (lower panel) in Funka Bay, southwestern Hokkaido, Japan, from December 2018 to December 2019. Crosses for the NBSS slope indicate the insignificance of the NBSS. The box at the bottom represents the period of the spring phytoplankton bloom in Funka Bay (cf. Fig. 2d).

ture within the zooplankters, high temperatures and low primary productivity, energy transfer to the higher trophic-levels (e.g. fishes) is expected to be small from summer to autumn.

For zooplankton in Group B, which were observed during the cold season (December to February), the abundances of the seasonal supplemental zooplankton taxa (e.g. Thaliacea and *Noctiluca* for Group A or *E. bungii*, Polychaeta, *M. pacifica*, and *Neocalanus* spp. for Group C) were diminished, and only core zooplankton taxa (other Copepoda, Appendicularia, Chaetognatha, and benthic larvae) were present, albeit to a limited extent (Fig. 5a). These facts suggest that the zooplankton in Group B is a transitional zooplankton community between the warm zooplankton in Group A to the high productivity-correlated zooplankton in Group C. Since the primary productivity in the Funka Bay is low during the winter before the onset of the phytoplankton bloom (Kudo & Matsunaga 1999), and there is a die-o of expatriated warm-water zooplankton (Thaliacea and *Noctiluca* in Group A), the zooplankton taxa comprising transitional zooplankton Group B are expected to be limited.

NBSS

This study is the first attempt to evaluate the seasonal variation of the NBSS based on zooplankton biovolume in Funka Bay (Fig. 6). The NBSS is used as an index of productivity, transfer e ciency to the higher trophic levels, and predator-prey interactions in marine ecosystems (Herman & Harvey 2006, Marcolin et al. 2015a). The slope of the NBSS varies depending on the productivity, energy transfer e ciency, and predator-prey interactions (Zhou 2006, Zhou et al. 2009). Theoretically, a slope of −1 for the NBSS indicates a steady zooplankton community, a slope steeper than −1 indicates a low transfer e ciency, and a flat slope indicates a high transfer e ciency (Sprules & Munawar 1986). It should also be noted that a flat slope is attributable to a high abundance of large zooplankters (García-Comas et al. 2014, Soviadan et al. 2022). The NBSS intercept becomes large when either the overall biomass or the number of small organisms increases (Moore & Suthers 2006).

In Funka Bay, NBSS was significant for 16 occasions of 21 sampling dates (Fig. 6). The insignificant NBSS values were observed for a restricted zooplankton group (Group B) and season (January to March) (Fig. 6). The NBSS slopes in Funka Bay showed clear seasonality separated into three groups. Significantly flat slopes (−0.63 to −0.29) were observed for 11–17 April, then relatively steep slopes (−1.09 to −0.63) were observed for May to January, and then extremely flat slopes and insignificant NBSS from January to March (Fig. 8). This clear seasonality in the NBSS slope is informative from the viewpoint of energy transfer from primary production to higher trophic levels.

Primary productivity in Funka Bay is initiated by the spring phytoplankton bloom that occurred from the end of February to mid-April (Fig. 2d), and nearly half of the annual primary production is concentrated over this short period (Kudo & Matsunaga 1999). After the spring bloom, the NBSS slopes were significant but flat observed for 11–17 April (Fig. 6). The dominant zooplankton taxon at these dates was the large-sized appendicularian, *O. labradoriensis* (Fig. 4, Shiga 1985). Appendicularia have the ability to feed on small-sized particles by filtering feeding (Alldredge 1976, Flood 1991, Choe & Deibel 2008, Doubleday & Hopcroft 2015). *O. labradoriensis* has been reported to be an important food item for flatfish larvae in the Funka Bay during spring (Miyamoto et al. 1993, Hashimoto et al. 2011, Yamaoka et al. 2019). The high biovolumes, flat slopes of NBSS, and dominance of large-sized appendicularians suggest that energy transfer from primary production to higher trophic levels functions well during that period (mid-April).

On the other hand, the slopes of NBSS were relatively steep for the long remaining season: May-January. During these seasons, because of the steep slopes of NBSS, energy transfer to higher trophic levels is expected to be small. The dominance of carnivorous taxa: Chaetognatha and Cnidaria during these periods (Fig. 4) also suggests that the energy is consumed within the zooplankton community.

The slopes of the NBSS were extremely flat from late January to March (Fig. 6). These seasonal sequences in the NBSS slope may be interpreted that high energy transfer occurs during the high productivity season (mid-April). Then the energy is consumed within the zooplankton community and only minimal energy reaches the higher trophic levels from May to January. After that, the zooplankton community was pause in both size and taxa from January to March (Fig. 6). Because of the low productivity during this period (Kudo & Matsunaga 1999), low energy transport to the higher trophic levels must occur during that period.

A special finding of this study is a significant relationship was apparent between the slope and intercept of the NBSS (Fig. 7). The spread of points across the graph especially for each of the three zooplankton groups varied from each other (Fig. 7). For group C, the spread was especially broad. This may partly be an artifact due to the number of sample points (i.e. dates) being greatest for this group (9 of 21 dates). Slope-intercept combinations for Group C appeared to be clustered into two temporal periods-early dates with high primary productivity (11 April to 8 May) and the later period (12 May to 14 June). The Appendicularia-dominant early period is characterized by a high energy transfer to higher trophic levels (e.g. mid-April). After that, low energy transfer to higher trophic levels was the norm for Group C. The NBSS values of Group A suggested low energy transfer throughout all periods they occurred. For zooplankton Group B, strong vertical mixing in shallow Funka Bay in winter may prevent the initiation of a high primary productivity regime (Fig. 2). Under such conditions, the dominant taxa were few in number and bio-

Table 2. Comparison of the slope (a) of normalised biomass size spectra ($Y=aX+b$) of the mesozooplankton community reported from the neighbouring waters of Japan, as obtained from the present study in Funka Bay, southwestern Hokkaido.

Location/region	Latitude (˚N)	Depth (m)	Period (n)	Mesh size (μm)	Instrument	Slope	References
Mombetsu (Southern Okhotsk Sea)	44°20′	0–8	Year-round (105)	335	OPC	−1.52 to −0.85	Hikichi et al. (2018)
Neighboring waters of Japan	20°20′–45°20′	0–150	May–August (78)	335	OPC	−1.24 to −0.90	Sato et al. (2015)
North Pacific (eight latitudinal transects)	35°00′–60°00′	0–150	May–August (1396)	335	OPC	−1.08 to −0.49	Shiota et al. (2013)
Central North Pacific (180° latitudinal transect)	35°00′–51°00′	0–150	June (444)	335	OPC	−0.81 to −0.55	Fukuda et al. (2012)
NW Pacific (three latitudinal transects)	35°00′–46°00′	0–150	July–August (86)	335	OPC	−0.75 to −0.42	Mishima et al. (2019)
Funka Bay	42°16′	0–87	Year-round (21)	100	ZooScan	−1.09 to −0.30	This study

(n) indicates the number of samples examined. Note that di erences in methodology (net mesh size and instrument) occurred. To make an adequate comparison with previous studies, we treated the same size range (0.35–5.00 mm) and applied the same size interval (every 0.05 mm) for the calculation of NBSS in this study.

mass for zooplankton Group B. The low zooplankton taxa and size ranges may have led to the lack of a significant NBSS for zooplankton Group B.

For a regional comparison, previously reported slopes of the NBSS based on the biovolume of zooplankton in the seas around Japan and the subarctic Pacific are summarised in Table 2. Several studies have compared seasonal changes in NBSS within the regions. The slope of the NBSS at Mombetsu Harbour in the southern Okhotsk Sea has been reported to be −0.85 to −1.1 during the period from January to April, while it increases to −1.31 to −1.52 during the period between May and December (Hikichi et al. 2018). The slope of the NBSS at 35–44°N along the 155°E line in the western Pacific has been reported as −0.90 in May, steepening to −1.11 to −1.24 in July and August (Sato et al. 2015). These results indicate that the slope of the NBSS is flat during the spring phytoplankton bloom period but becomes steeper after summer. Such seasonally changing patterns in the NBSS slope correspond with the results of this study in Funka Bay.

Regional patterns of NBSS slopes are flat in the transitional region but steep in the subarctic and subtropical regions, as has been reported for latitudinal transects in the North Pacific (Fukuda et al. 2012, Shiota et al. 2013). Annually changing patterns in NBSS slopes have also been reported for latitudinal transects in the western North Pacific (Mishima et al. 2019). Through comparison with those reported values of NBSS slopes for the seas around Japan and the subarctic Pacific, the NBSS slopes in Funka Bay are characterised as flatter than previously reported slopes. In particular, the flattest slope of the NBSS observed in this study (−0.32) is beyond the range of other studies. This flat slope is an indicator of high energy transfer e ciency to higher trophic level organisms (Sprules & Munawar 1986). This suggests that Funka Bay, located in a coastal area, has more e cient energy transfer to higher trophic level organisms than in oceanic regions.

While these findings are interesting, it should be noted that the previous reports applied a di erent methodology: zooplankton samples were collected by a 335-μm mesh size net, and the biovolume data were quantified by OPC. Since we collected zooplankton samples using a 100-μm mesh size net and obtained imaging data by ZooScan, differences in methodology may have a ected the results. However, we applied the same size ranges for analysing NBSS as in the previous studies (350 to 5000 μm). Since we applied the same size ranges for the estimation of NBSS, the results obtained in this study should make a comparison possible with previous studies.

OPC is an instrument capable of counting and sizing zooplankton and simultaneously measuring light attenuation (Herman 1988). Contrastingly ZooScan can capture images of the zooplankton contained in the sample, and both size and taxonomic information become analysable (Gorsky et al. 2010). Since ZooScan can also obtain taxonomic information from the samples, ZooScan may be superior to OPC. However, during the mounting of zooplankton on the ZooScan frame, the spreading of fragile zooplankton bodies (e.g., jellyfishes) may lead to an overestimate of their biovolume (Naito et al. 2019). Additionally, the accuracy of OPC data is compromised by contamination from the non-living fraction (e.g. detritus), and size underestimations may occur for taxa with slender bodies (e.g. Chaetognatha) or with transparent bodies (e.g. jellyfishes) (Yokoi et al. 2008). In the future, considering these characteristics of optical and imaging instruments, it will be necessary to accumulate information on zooplankton size and structure in various locations and obtain general patterns for the geographical and seasonal changes in zooplankton size structure to clarify the factors that a ect zooplankton size and composition.

Acknowledgements

We thank the captains, o cers, crews, and researchers onboard the T/S *Ushio-Maru*, Hokkaido University, for their great e orts during the field sampling. This work was supported by the Arctic Challenge for Sustainability II (ArCS II) Program (Grant Number JPMXD1420318865); the Environment Research and Technology Development Fund (JPMEERF20214002) of the Environmental Restoration and Conservation Agency of Japan; and Grants-in-Aid for Challenging Research (Pioneering) (JP20K20573) and Scientific Research (JP22H00374 (A), JP21H02263

(B), JP20H03054 (B), JP19H03037 (B), and JP17H01483 (A)) from the Japan Society for the Promotion of Science (JSPS).

References

Alldredge AL (1976) Field behavior and adaptive strategies of appendicularians. Mar Biol 38: 29–39.

Ara K, Nakamura S, Takahashi R, Shiomoto A, Hiromi J (2013) Seasonal variability of the red tide-forming heterotrophic dinoflagellate *Noctiluca scintillans* in the neritic area of Sagami Bay, Japan: its role in the nutrient-environment and aquatic ecosystem. Plankton Benthos Res 8: 9–30.

Arima D, Yamaguchi A, Abe Y, Matsuno K, Saito R, Asami H, Shimada H, Imai I (2014a) Seasonal changes in zooplankton community structure in Ishikari Bay, Japan Sea. Bull Fish Sci Hokkaido Univ 64: 17–23.

Arima D, Yamaguchi A, Abe Y, Matsuno K., Saito R, Asami H, Shimada H, Imai I (2014b) Seasonal changes in size and oil sac volume of three planktonic copepods, *Paracalanus parvus* (Claus, 1863), *Pseudocalanus newmani* Frost, 1989 and *Oithona similis* Claus, 1866, in a temperate embayment: what controls their seasonality? Crustaceana 87: 364–375.

Ban S, Miyagawa Y, Okuda Y, Shiga N (1998) Succession of the calanoid copepod community in Funka Bay during spring phytoplankton bloom. Mem Fac Fish Hokkaido Univ 45: 42–47.

Choe N, Deibel D (2008) Temporal and vertical distributions of three appendicularian species (Tunicata) in Conception Bay, Newfoundland. J Plankton Res 30: 969–979.

Dohi K (1982) Seasonal change of tintinnid community in Funka Bay. Bull Plankton Soc Japan 29: 77–87. (in Japanese with English abstract)

Doubleday AJ, Hopcroft RR (2015) Interannual patterns during spring and late summer of larvaceans and pteropods in the coastal Gulf of Alaska, and their relationship to pink salmon survival. J Plankton Res 37: 134–150.

Ducklow HW, Steinberg DK, Buesseler KO (2001) Upper ocean carbon export and the biological pump. Oceanogr 14: 50–58.

Flood PR (1991) Architecture of, and water circulation and flow rate in, the house of the planktonic tunicate *Oikopleura labradoriensis*. Mar Biol 111: 95–111.

Fukuda J, Yamaguchi A, Matsuno K, Imai I (2012) Interannual and latitudinal changes in zooplankton abundance, biomass and size composition along a central North Pacific transect during summer: analyses with an Optical Plankton Counter. Plankton Benthos Res 7: 64–74.

García-Comas C, Chang C-Y, Ye L, Sastri AR, Lee Y-C, Gong G-C, Hsieh C-h (2014) Mesozooplankton size structure in response to environmental conditions in the East China Sea: How much does size spectra theory fit empirical data of a dynamic coastal area? Prog Oceanogr 121: 141–157.

Gorsky G, Ohman MD, Picheral M, Gasparini S, Stemmann L, Romagnan J, Cawood A, Pesant S, Garcia-Comas C, Prejger F (2010) Digital zooplankton image analysis using the ZooScan integrated system. J Plankton Res 32: 285–303.

Hashimoto Y, Maeda A, Oono Y, Kano Y, Takatsu T (2011) Feeding habits of two-flatfish-species larvae in Funka Bay, Japan —importance of *Oikopleura* as prey—. Bull Plankton Soc Japan 58: 165–177. (in Japanese with English abstract)

Herman AW (1988) Simultaneous measurement of zooplankton and light attenuance with a new optical plankton counter. Cont Shelf Res 8: 205–221.

Herman AW, Harvey M (2006) Application of normalized biomass size spectra to laser optical plankton counter net inter comparisons of zooplankton distributions. J Geophys Res 111: C05S05.

Hikichi H, Arima D, Abe Y, Matsuno K, Hamaoka S, Katakura S, Kasai H, Yamaguchi A (2018) Seasonal variability of zooplankton size spectra at Mombetsu Harbour in the southern Okhotsk Sea during 2011: An analysis using an optical plankton counter. Reg Stud Mar Sci 20: 34–44.

Hirakawa K (1976) Seasonal change of population structure of a boreal oceanic copepod, *Eucalanus bungii bungii* Johnson in Funka Bay, Hokkaido, Japan. Bull Fac Fish Hokkaido Univ 27: 71–77. (in Japanese with English abstract)

Hirakawa K (1979) Seasoal change of population structure of a calanoid copepod, *Calanus pacificus*, in Funka Bay, Hokkaido. Bull Plankton Soc Japan 26: 49–58. (in Japanese with English abstract)

Hirakawa K (1983) Seasonal distribution of the planktonic copepods, and life histories of *Calanus pacificus*, *Calanus plumchrus* and *Eucalanus bungii bungii* in the waters of Funka Bay, southern Hokkaido, Japan. PhD thesis. Hokkaido Univ. (in Japanese)

Hirakawa K, Kaga T, Sato T, Kasai H (2019) Regional characteristics of zooplankton as food for juvenile chum salmon *Oncorhynchus keta* in the coastal waters around Hokkaido, with special reference to copepod community structure. Bull Plankton Soc Japan 66: 72–85. (in Japanese with English abstract)

Kamba M (1977) Feeding habits and vertical distribution of walleye pollock, *Theragra chalcogramma* (Pallas), in early life stage in Uchiura Bay, Hokkaido. Res Inst North Pac Fish Hokkaido Univ Spec. Vol.: 175–197.

Kida S, Takayama K, Sasaki YN, Matsuura H, Hirose N (2021) Increasing trend in Japan Sea Throughflow transport. J Oceanogr 77: 145–153.

Kitamura M, Nakagawa Y, Nishino Y, Segawa S, Shiomoto A (2016) Comparison of the seasonal variability in abundance of the copepod *Pseudocalanus newmani* in Lagoon Notoro-ko and a coastal area of the southwestern Okhotsk Sea. Polar Sci 15: 62–74.

Kudo I, Matsunaga K (1999) Environmental factors a ecting the occurrence and production of the spring phytoplankton bloom in Funka Bay, Japan. J Oceanogr 55: 505–513.

Marcolin CR, Gaeta S, Lopes RM (2015a) Seasonal and interannual variability of zooplankton vertical distribution and biomass size spectra o Ubatuba, Brazil. J Plankton Res 37: 808–819.

Marcolin CR, Lopes RM, Jackson GA (2015b) Estimating zooplankton vertical distribution from combined LOPC and ZooScan observations on the Brazilian Coast. Mar Biol 162: 2171–2186.

van der Meeren T, Næss T (1993) How does cod (*Gadus morhua*) cope with variability in feeding conditions during early larval

stage? Mar Biol 116: 637–647.
Michaels AF, Silver MW (1988) Primary production, sinking fluxes and microbial food web. Deep-Sea Res 35A: 473–490.
Mishima K, Matsuno K, Yamaguchi A (2019) Zooplankton size structure in the summer western North Pacific Ocean: Analysis by optical plankton counter. Bull Fish Sci Hokkaido Univ 69: 37–45. (in Japanese with English abstract)
Miyaguchi H, Fujiki T, Kikuchi T, Kuwahara VS, Toda T (2006) Relationship between the bloom of *Noctiluca scintillans* and environmental factors in the coastal waters of Sagami Bay, Japan. J Plankton Res 28: 313–324.
Miyamoto T, Takatsu T, Nakatani T, Maeda T, Takahashi T (1993) Distribution and food habits of eggs and larvae of *Hippoglossoides dubius* in Funka Bay and its o shore waters, Hokkaido. Fish Oceanogr 57: 1–14.
Moore SK, Suthers IM (2006) Evaluation and correction of subresolved particles by the optical plankton counter in three Australian estuaries with pristine to highly modified catchments. J Geophys Res 111: C05S04.
Naito N, Abe Y, Matsuno K, Nishizawa B, Kanna N, Sugiyama S, Yamaguchi A (2019) Surface zooplankton size and taxonomic composition in Bowdoin Fjord, north-western Greenland: A comparison of ZooScan, OPC and microscopic analyses. Polar Sci 19: 120–129.
Nakatani T (1988) Studies on the early life history of walleye pollock *Theragra chalcogramma* in Funka Bay and vicinity, Hokkaido. Mem Fac Fish Hokkaido Univ 35: 1–46.
Nakatani T (2016) Year class strength and early life history of the Pacific population of walleye pollock, *Gadus chalcogrammus*, in Japan. Mem Fac Fish Hokkaido Univ 58: 1–11.
Nakatani T (2017) Relationship between hydrographic conditions in Funka Bay, Hokkaido, during winter and year class strength of the Japanese Pacific population of walleye pollock *Gadus chalcogrammus* from 1991 to 2013. Mem Fac Fish Sci Hokkaido Univ 59: 19–43. (in Japanese with English abstract)
Nakatani T, Maeda T (1993) Early life history of walleye pollock. Sci Rep Hokkaido Fish Exp Stn 42: 15–22. (in Japanese with English abstract)
Ohtani K (1971) Studies on the change of the hydrographic conditions in the Funka Bay II. Characteristics of the waters occupying the Funka Bay. Bull Fac Fish Hokkaido Univ 22: 58–66. (in Japanese with English abstract)
Ooki A, Shida R, Otsu M, Onishi H, Kobayashi N, Iida T, Nomura D, Suzuki K, Yamaoka H, Takatsu T (2019) Isoprene production in seawater of Funka Bay, Hokkaido, Japan. J Oceanogr 75: 485–501.
Picheral M, Colin S, Irisson J-O (2017) EcoTaxa, a tool for the taxonomic classification of images. http://ecotaxa.obs-vlfr.fr. (accessed in 11 June 2022)
Platt T, Denman K (1977) Organization in pelagic ecosystem. Helgoländ wiss Meer 30: 575–581.
Platt T, Denman K (1978) The structure of pelagic marine ecosystems. Rapp P-v Réun Cons Int Explor Mer 173: 60–65.
Romagnan J-B, Legendre L, Guidi L, Jamet J-L, Jamet D, Mousseau L, et al. (2015) Comprehensive model of annual plankton succession based on the whole-plankton time series approach. PLoS ONE 10: e0119219.
Romagnan JB, Aldamman L, Gasparini S, Nival P, Aubert A, Jamet JL, Stemmann L (2016) High frequency mesozooplankton monitoring: Can imaging systems and automated sample analysis help us describe and interpret changes in zooplankton community composition and size structure—An example from a coastal site. J Mar Syst 162: 18–28.
Sasaoka K, Saitoh S-i, Ban S, Kudo I, Miyake H (1998) Coastal Oyashio Multidisciplinary and Advanced Study (COMPAS) Program using new ocean color remote sensing and intensive ship observations. Mem Fac Fish Hokkaido Univ 45: 11–17.
Sato K, Matsuno K, Arima D, Abe Y, Yamaguchi A (2015) Spatial and temporal changes in zooplankton abundance, biovolume, and size spectra in the neighboring waters of Japan: analyses using an optical plankton counter. Zool Stud 54: 1–15.
Sheldon RW, Sutcli e WHJr, Paranjape MA (1977) Structure of pelagic food chain and relationship between plankton and fish production. J Fish Res Bd Can 34: 2344–2353.
Shiga N (1985) Seasonal and vertical distributions of Appendicularia in Volcano Bay, Hokkaido, Japan. Bull Mar Sci 37: 425–439.
Shimada H, Sakaguchi K, Mori Y, Watanobe M, Itaya K, Asami H (2012) Seasonal and annual changes in zooplankton biomass and species structure in four areas around Hokkaido (Doto and Donan areas of the North Pacific, the northern Japan Sea and the southern Okhotsk Sea). Bull Plankton Soc Japan 59: 63–81. (in Japanese with English abstract)
Shinada A, Shiga N, Ban S (1999a) Structure and magnitude of diatom spring bloom in Funka Bay, southwestern Hokkaido, Japan, as influenced by the intrusion of Coastal Oyashio Water. Plankton Biol Ecol 46: 24–29.
Shinada A, Shiga N, Ban S (1999b) Origin of *Thalassiosira* diatoms that cause the spring phytoplankton bloom in Funka Bay, southwestern Hokkaido, Japan. Plankton Biol Ecol 46: 89–93.
Shiota T, Abe Y, Saito R, Matsuno K, Yamaguchi A, Imai I (2013) Spatial changes in mesozooplankton community structure in the North Pacific: Analyses by optical plankton counter. Bull Fish Sci Hokkaido Univ 63: 13–22. (in Japanese with English abstract)
Soviadan YD, Benedetti F, Brandão MC, Ayata S-D, Irisson J-O, Jamet JL, Kiko R, Lombard F, Gnandi K, Stemmann L (2022) Patterns of mesozooplankton community composition and vertical fluxes in the global ocean. Prog Oceanogr 200: 102717.
Sprules WG, Munawar M (1986) Plankton size spectra in relation to ecosystem productivity, size, and perturbation. Can J Fish Aquat Sci 43: 1789–1986.
Suzuki T, Yamamoto K, Narasaki T (2013) Predation pressure of *Noctiluca scintillans* on diatoms and thecate dinoflagellates o the western coast of Kyushu, Japan. Plankton Benthos Res 8: 186–190.
Vandromme P, Stemmann L, Garcìa-Comas C, Berine L, Sun X, Gorsky G (2012) Assessing biases in computing size spectra of automatically classified zooplankton from imaging systems: A case study with the ZooScan integrated system. Methods Oceanogr 1–2: 3–21.
Vandromme P, Nogueira E, Huret M, Lopez-Urrutia Á, González-Nuevo González G, Sourisseau M, Petitgas P (2014) Springtime zooplankton size structure over the continental shelf of the Bay of Biscay. Ocean Sci 10: 821–835.
Welschmeyer NA (1994) Fluorometric analysis of chlorophyll *a*

in the presence of chlorophyll *b* and pheopigments. Limnol Oceanogr 39: 1985–1992.

Yamaguchi A, Shiga N (1997) Vertical distributions and life cycles of *Pseudocalanus minutus* and *P. newmani* (Copepoda; Calanoida) o Cape Esan, southwestern Hokkaido. Bull Plankton Soc Japan 44: 11–20. (in Japanese with English abstract)

Yamaguchi A, Miwa Y, Inoue K, Matsumoto T, Shiga N (2003) Characteristics of zooplankton community in the coastal Oyashio water. Bull Coast Oceanogr 41: 23–31. (in Japanese with English abstract)

Yamaguchi A, Matsuno K, Abe Y, Arima D, Ohgi K (2014) Seasonal changes in zooplankton abundance, biomass, size structure and dominant copepods in the Oyashio region analysed by an optical plankton counter. Deep-Sea Res I 91: 115–124.

Yamaoka H, Takatsu T, Suzuki K, Kobayashi N, Ooki A, Nakaya M (2019) Annual and seasonal changes in the assemblage of planktonic copepods and appendicularians in Funka Bay before and after intrusion of Coastal Oyashio Water. Fish Sci 85: 1077–1087.

Yokoi Y, Yamaguchi A, Ikeda T (2008) Regional and inter-annual changes in the abundance, biomass and community structure of mesozooplankton in the western North Pacific in early summer: as analyzed with an optical plankton counter. Bull Plankton Soc Japan 55: 79–88. (in Japanese with English abstract)

Yokouchi K (1985) Reproduction and larval ecology of the sandworm *Neanthes virens* (Sars) from the southern Hokkaido. Bull Plankton Soc Japan 32: 1–13.

Zhou M (2006) What determines the slope of a plankton biomass spectrum? J Plankton Res 28: 437–448.

Zhou M, Tande K S, Zhu Y, Basedow S (2009) Productivity, trophic levels and size spectra of zooplankton in northern Norwegian shelf regions. Deep-Sea Res II 56: 1934–1944.